A Rheo-optical Study of Stress−Fluctuations Coupling in a Disordered and Entangled Diblock Copolymer Solution

Loic Hilliou,*,† Dimitris Vlassopoulos,‡,§ Stergios Pispas,|| and Nikos Hadjichristidis⊥

REQUIMTE, Faculty of Engineering, University of Porto, Rua Dr. Roberto Frias, s/n, 4200-465 Porto, Portugal; FORTH-Institute of Electronic Structure and Laser, P.O. Box 1527, 71110 Heraklion, Crete, Greece; Department of Materials Science and Technology, University of Crete, P.O. Box 2208, 710 03 Heraklion, Crete, Greece; Theoretical and Physical Chemistry Institute, National Hellenic Research Foundation, 48 Vass. Constantinou Ave., 11635 Athens, Greece; and Department of Chemistry, University of Athens, 15701 Zografou, Athens, Greece

Received November 19, 2007; Revised Manuscript Received February 29, 2008

ABSTRACT: We report on rheo-optical experiments performed with an entangled asymmetric polystyrene−polyisoprene diblock copolymer solution in dioctyl phthalate (DOP), in the regime of pretransitional fluctuations. The combined information extracted from optical signals under steady and transient flows suggests the stress enhancement of fluctuations in the flow direction and their subsequent suppression at higher stresses in the plane normal to the velocity gradient direction. The viscoelastic signature of these structural changes resulting from the complex interplay between fluctuations and the shear flow includes an initial shear thinning regime followed by an abrupt shear thickening and then an apparent viscosity plateau. At even higher stresses, the flow curve displays a second shear thinning, and eventually a second viscosity plateau is reached. The corresponding optical response indicates that the copolymer solution is driven toward a dynamic phase separation, in a way similar to a semidilute polymer solution sheared below the theta point. However, no flow instability is detected at the highest stresses because the shear-induced structure relaxes too fast when compared to the longest relaxation time exhibited by the quiescent disordered copolymer solution.

I. Introduction

A promising route to the production of innovative high added-value soft materials with new nanosized morphologies is their controlled processing.[1] In order to achieve this goal, a fundamental understanding of the coupling between external fields such as shear stress and the induced morphology of structurally complex fluids is a prerequisite to any engineering strategy. This line of research has received a great deal of attention in the past two decades, as new experimental tools combining rheometry with in-situ structural characterization (optical polarimetry and microscopy, light, X-ray or neutron scattering, NMR spectroscopy) are now easier to implement.[2–5]

It is widely known that shear flow can shift the phase boundaries of different systems. For example, a rich literature is now available that reports on experimental[6–8] and theoretical[9,10] description of the shear-induced phase separation in semidilute entangled polymer solutions. When sheared below the theta point, these solutions exhibit a shear thinning behavior, accompanied by the appearance of turbidity and linear conservative dichroism, in contrast to their usually transparent appearance at rest. These features signify the anisotropic shear enhancement of concentration fluctuations (polymer-rich domains in a solvent-rich matrix) which is related to the so-called "butterfly" pattern in light scattering.[8] At higher shear rates, the polymer-rich domains rearrange in a stringlike morphology oriented along the flow and give rise to a shear thickening. In order to better characterize this counterintuitive high shear regime, we recently performed stress controlled rheo-optical experiments[11] on a semidilute polystyrene solution. The coupling between stress and concentration fluctuations resulted in time-periodic signals in both mechanical and optical responses, which were related to the formation and disruption of macroscopic rings made of polymer-rich phase-separated domains with dimensions on the order of the sample thickness. Similar rheo-optical periodic patterns were obtained with lyotropic lamellar systems[12] and wormlike surfactant solutions[13] undergoing a shear banding instability characterized by a shear rate plateau in the flow curve.

Here, we address the coupling between stress and concentration fluctuations in a semidilute entangled diblock copolymer solution. This system differs from its homopolymer counterpart[11] by the presence of additional enthalpic interactions between unlike block sequences. Under quiescent conditions, these interactions force the system to undergo a disorder-to-order transition[14] (DOT) with decreasing temperature or increasing copolymer concentration. Shear flow is known to affect this transition. For instance, the shear-induced isotropic-to-lamellar transition in diblock copolymers melts and solutions has been predicted[15,16] and experimentally observed.[17–20] At temperatures and concentrations corresponding to the isotropic disordered state, but close enough to the ordering transition, concentration fluctuations are large[21] and their lifetime is slow enough to be affected by the mechanical field: above a critical shear rate, flow suppresses the fluctuations, inducing a macroscopic order at temperatures higher than the quiescent ordering transition temperature. However, the rheological signature of the shear-induced DOT has been less documented[22] than the mechanical patterns associated with the shear-induced lamellae orientations,[23–25] and most experimental studies were conducted under large-amplitude oscillatory shear or shear rate-controlled conditions. It is likely that phenomena such as orientation of ordered phases can be induced under stress-controlled conditions, as suggested by a recent phenomenological model[26] which predicts that different flow curve−structure relationships can be obtained depending on whether shear stress or shear rate is imposed on a complex fluid. Furthermore, the coupling between the shear-induced morphology and the mechanical field still needs to be

* Corresponding author: Fax (+351) 22 508 1449; Ph (+351) 22 508 1686; e-mail: hilliou@fe.up.pt.
† University of Porto.
‡ FORTH-Institute of Electronic Structure and Laser.
§ University of Crete.
|| National Hellenic Research Foundation.
⊥ University of Athens.

10.1021/ma702566n CCC: $40.75
Published on Web 04/19/2008

explored. For instance, a shear-induced order to disorder transition (ODT) has been observed[20] for shear rates higher than the critical one needed to achieve a shear-induced DOT. This shear-induced disordering (a kind of re-entrant behavior) is not accounted for by theories describing the behavior of diblock copolymers undergoing a flow field.[15,16]

In this paper, we report on rheo-optical experiments (flow-induced dichroism and birefringence) performed over a range of shear stresses, thus extending the previous works by providing a rheological characterization of the shear-induced structures under controlled stress conditions and by exploring the flow regime where the shear-induced morphology is further stressed. In this regime, an additional coupling between stress and concentration fluctuations arises as experiments are carried out below the theta temperature for the polystyrene blocks. We show that the enthalpic interactions of the polystyrene and the polyisoprene blocks in the copolymer solution lead to a much more complicated but at the same time much richer dynamic behavior than the one observed for the polystyrene solution:[11] the flow curve is rather complex and can be described by five regimes as a function of shear stress. A low-stress Newtonian plateau (regime A) is followed by a strong shear thinning (regime B) where concentration fluctuations are enhanced along the flow direction, as demonstrated by the development of flow induced linear conservative dichroism. A shear thickening takes place afterward (regime C) and correlates with the disappearance of the dichroism signal, which suggests the disordering and breakup of spatial correlation of the ordered phase developed in the vorticity−flow plane. A further increase in the shear stress results in a second shear thinning (regime D), and eventually the flow curve displays a second viscosity plateau (regime E). These high-stress regimes (D and E) relate to dichroism signals reminiscent of data obtained with a semidilute polystyrene solution below the theta temperature. However, the absence of any time and spatial periodicity in both mechanical and optical signals indicates that the flow instability associated with a non-steady-shear banding structure traveling along the vorticity direction and evidenced in the polymer solution under similar stress conditions cannot develop in the diblock copolymer solution. A recent minimal model for shear thickening fluids with long structural memory[27] suggests that the absence of flow instability is related to the fast relaxation of the shear-induced structure which occurs on a time scale shorter than the stress relaxation of the quiescent disordered copolymer solution. By merging optical and rheological experiments, we aim here at providing a roadmap for studying such complex fluids. The combined information extracted from optical signals under steady and transient flows is also suggestive of ways for rheology control in systems with enthalpic interactions.

The paper is organized as follows. In the next section, experimental details are provided, whereas results are presented in section III. In section III.1, we start by assessing the temperature regime corresponding to concentration fluctuations in the quiescent copolymer solution, and we present the flow curve along with the five stress regimes. Following this, each stress regime is studied in dedicated subsections, where optical data, namely the dichroism and birefringence recorded during stress sweeps and separate rheo-optical transients, are presented. In addition, the rheo-optical patterns of regimes D and E are compared with those of a polystyrene semidilute solution sheared under the theta point. Results are then discussed in section IV: data are analyzed in light of theoretical arguments,[28] and comparison with reports on fluids undergoing shear-induced phase transition, phase separation, or flow instability is provided. In addition, the discrepancies observed between the copolymer solution and the polystyrene solution are rationalized by a recent model.[27] Finally, the picture emerging from the flow−fluctuations couplings is summarized, and some concluding remarks are provided in section V.

Scheme 1. Definition of Mechanical Field Directions and of the Dichroism Orientation Angle θ''

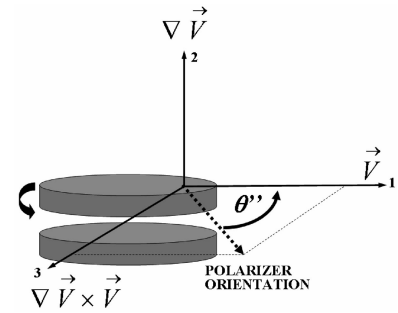

II. Experimental Section

II.1. Materials. A high molecular mass ($M_w = 1.6 \times 10^6$ g/mol) and nearly monodisperse ($M_w/M_n = 1.15$) asymmetric polystyrene−polyisoprene diblock copolymer (PS-*b*-PI) was synthesized by anionic polymerization as described elsewhere.[29,30] The mass fraction f of the polystyrene block was 85%, as determined by proton NMR spectroscopy. An appropriate amount of this copolymer was dissolved in dioctyl phtalate (DOP) in order to reach a concentration of 8 wt %. This concentration corresponds to roughly seven entanglements of the polystyrene block and four entanglements of the polyisoprene block. The PS-*b*-PI solution was prepared by slow stirring using dichloroethane as a cosolvent. The latter was subsequently removed by gradual evaporation at room temperature under vacuum, until constant weight was reached.

For comparison, a semidilute polymer solution, similar to the one used in an earlier paper,[11] was also prepared: a high molecular mass ($M_w = 2 \times 10^6$ g/mol, polydispersity index $M_w/M_n = 1.15$) polystyrene sample (PS) obtained from Polymer Source, Canada, was dissolved in DOP at a concentration of 8 wt %. This concentration corresponds to roughly 25 effective entanglements. This polymer solution is thereafter referred as PS-DOP.

II.2. Optical and Mechanical Rheometry. A Rheometric Scientific constant-stress rheometer (DSR-200) was used and coupled with an optical train described in length elsewhere.[31,32] The latter allows the modulation (at 50 kHz) of a linearly polarized laser light, which is traveling through the sample sheared between the two parallel quartz plates (diameter 38.1 mm) in the rheometer. The polarization of the transmitted light is then analyzed by means of a photodiode connected to two lock-in amplifiers locked at the first and the second harmonics of the modulation. These harmonics give signals proportional to $-\sin 2\theta'' \, \Delta n''_{13}$ and $\cos 2\theta'' \, \Delta n''_{13}$, respectively, where $\Delta n''_{13}$ stands for the dichroism probed in the plane made by the vorticity and the flow directions and θ'' is the dichroism orientation angle with respect to the polarizer direction, namely the bisector of the angle made by flow and vorticity directions (see Scheme 1). $\Delta n''_{13}$ and its orientation with respect to the shear direction are then easily computed from these two signals. Note here that due to symmetry considerations, the dichroism orientation is either along the vorticity or the flow direction,[2] and θ'' reads values close to either −45° or 45°, respectively.[33] Shear-induced birefringence $\Delta n'_{13}$ and its orientation angle θ' were measured in a similar way, a circular polarizer being simply inserted in front of the photodiode. In the signal analysis of the birefringence, it is further assumed that dichroism is small compared to birefringence. The validity of the assumption is demonstrated for the whole range of applied stresses by comparing Figures 3 and 4 (see below).

The two PS-*b*-PI copolymer and PS solutions were submitted to steady stress sweep tests, where each stress step was applied during 60 s and shear rate was measured during the last second of the step. This step duration is long enough to reach steady-state conditions and to ensure probing steady-state shear rates and

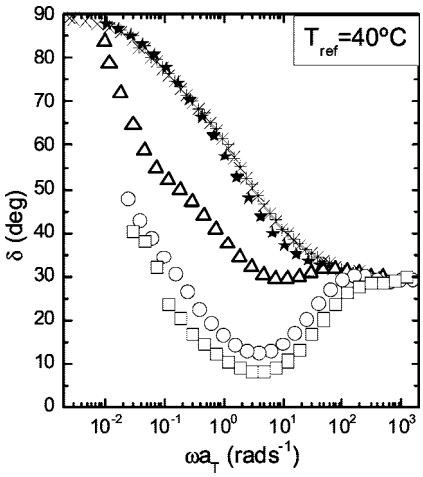

Figure 1. Phase angle as a function of the reduced frequency for the PS-*b*-PI solution at temperatures 40 °C (+), 30 °C (×), 25 °C (*), 20 °C (★), 15 °C (Δ), 10 °C (○), and 8 °C (□).

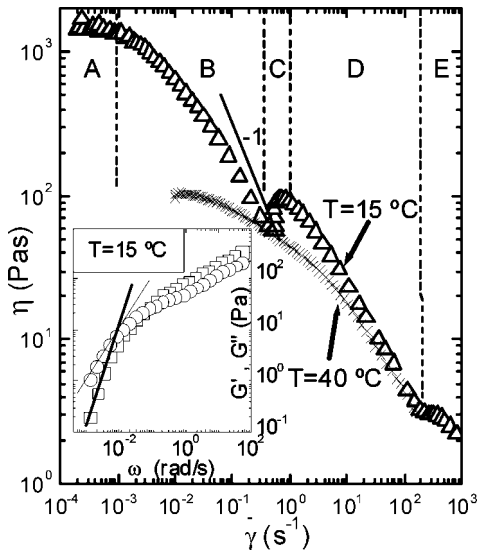

Figure 2. Shear rate dependent viscosity of the PS-*b*-PI copolymer solution measured during steady stress sweep tests performed (60 s shearing for each stress step) at two temperatures: (×) 40 °C and (Δ) 15 °C; the solid line indicates a power law with exponent −1, whereas the vertical dotted lines indicate the separations between the different flow regimes A, B, C, D, and E. Inset: dynamic frequency sweep at 15 °C showing the storage (G', □) and loss (G'', ○) moduli; solid lines have slopes 1 (for G'') and 2 (for G'), and their intersection determines the inverse longest relaxation time.

viscosities, as inferred from creep tests performed prior to the sweeps. Examples of such rheological transients are given in Figures 5 and 7 and show that the shear rate response has reached a steady plateau within 60 s after the stress start-up. Note that the reported shear rate values refer to the rim values in the present parallel-plates setup; the actual shear rate values at the point where optical data are simultaneously recorded are lower by a factor of 0.84. For complementary information, additional small-amplitude frequency sweep tests, step rate tests, and subsequent shear and normal stresses relaxation experiments were carried out using a Rheometric Scientific ARES rheometer equipped with a 100FRTN1-HR transducer and a cone and plate geometry (diameter 25 mm, cone angle 0.04 rad). These tests showed good reproducibility with rheo-optical experiments (see Figure 3 and section III.1), thus confirming that the nonuniform shear rate along the vorticity axis of the parallel plates used in the rheo-optical setup does not qualitatively interfere with the reported results. Therefore, the viscosity data obtained with the parallel plates were not processed further, as within the accuracy of the measurements for the range of rates probed there was no

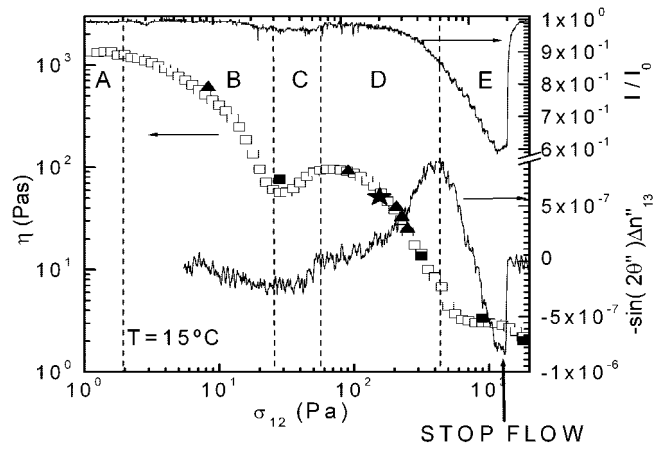

Figure 3. Transmitted light (normalized with I_0, the light transmitted by the quiescent PS-*b*-PI solution), dichroism first harmonic, and steady-state viscosity recorded in situ at $T = 15$ °C during the stress sweep test displayed in Figure 2. The vertical arrow and the STOP FLOW notation indicate the flow cessation followed by the fast relaxation of the optical signal. Vertical dotted lines indicate the separation between the five flow regimes. Solid symbols refer to steady-state viscosity data obtained with different shearing geometries (see text).

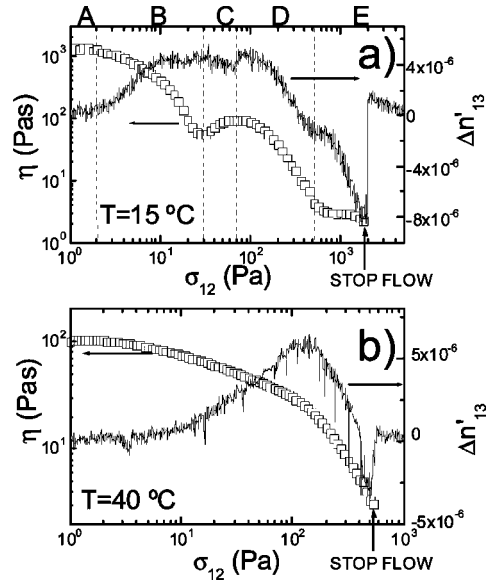

Figure 4. Steady-state rheo-optical response at (a) $T = 15$ °C and (b) $T = 40$ °C: viscosity−stress rheogram and corresponding stress birefringence measured in situ. Each data point in the viscosity curves was obtained after 60 s shearing at the corresponding stress. The vertical arrows with the STOP FLOW notations indicate the fast reorientation and subsequent slow relaxation. Vertical dotted lines indicate the separation between the five flow regimes.

evidence of noticeable effect of the nonhomogeneous shear field on the reported data. In addition, the optical signal is averaged over a small volume (the laser beam diameter is 0.8 mm) where the shear rate can be considered as constant. Additional polarized light microscopy under shear was performed using a Linkam CSS450 plate−plate shear cell (not shown).

III. Results

III.1. Concentration Fluctuations and Steady Flow Behavior. Figure 1 presents the phase shift angle, δ, between applied sinusoidal strain and measured sinusoidal stress (experiments performed with the ARES rheometer), as a function of the reduced frequency ωa_T for the PS-*b*-PI solution at different temperatures. This representation was preferred over the one

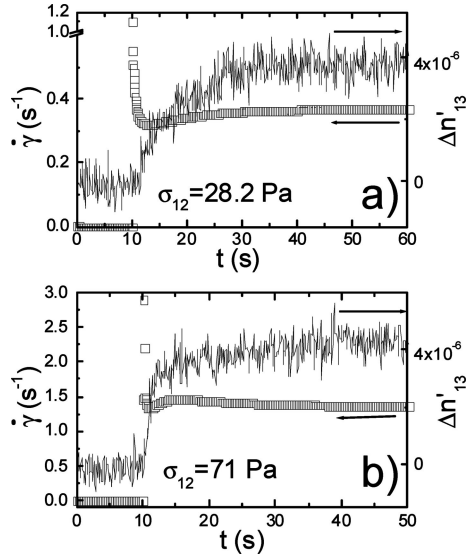

Figure 5. Shear rate (open squares) and birefringence transients measured at $T = 15$ °C during start of shear stress at (a) 28.2 Pa (this stress level corresponds to the separation between regimes B and C where form effects dominate the birefringence) and (b) at 71 Pa (end of the shear thickening regime).

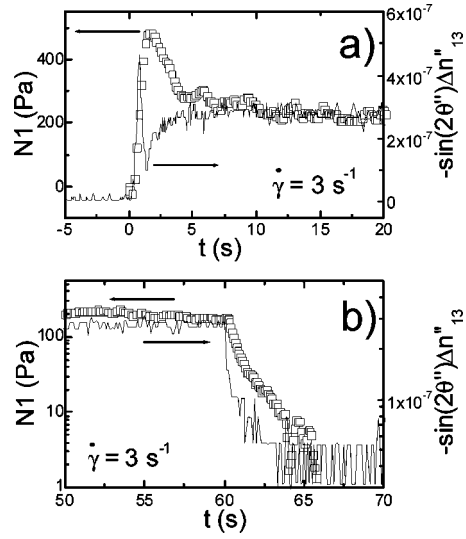

Figure 6. Normal stress N1 (□) and dichroism first harmonic transients measured at $T = 15$ °C during a start of shear (a) and upon flow cessation (b) for a shear rate of 3 s^{-1} corresponding to regime D.

displaying the frequency dependence of the dynamic shear moduli G' and G'' because it has been recognized[21] as particularly sensitive to deviations from thermorheological simplicity. For a disordered PS-*b*-PI copolymer solution, a viscous behavior is expected at low frequencies (the phase angle being 90°). Figure 1 shows that all data exhibit such a viscous-like terminal behavior. Furthermore, data collected at 30, 25, and 20 °C are well superposed onto the ones obtained at 40 °C. The three horizontal shift factors a_T used to obtain this superimposition are following a WLF temperature dependence with parameters $C_1 = 7.6$ and $C_2 = 88.6$ K, thus confirming the thermorheologically simple behavior of the PS-*b*-PI copolymer solution at temperatures above 20 °C. At lower temperatures an elastic-like process shows up as a local minimum in the otherwise monotonic frequency dependence of δ.

This process is responsible for the lack of superposition of data and is the rheological signature of concentration fluctuations.[21] We note however that in the high-frequency regime, where local copolymer chain dynamics is resolved, all data collapse into a single master curve. The horizontal shifting factors a_T, used to superpose the high-frequency part of curves obtained at 15, 10, and 8 °C onto the reference curve obtained at $T_{ref} = 40$ °C, are not following the WLF behavior observed at higher temperatures. The departure from simple WLF behavior near a transition is in qualitative agreement with earlier data obtained with liquid crystalline polymers at temperatures corresponding to the isotropic and nematic phases.[34,35] Both thermorheologically complex behavior evidenced below 20 °C and elastic-like relaxation process are consistent with theories predicting the contributions of fluctuations to the dynamic viscoelastic functions near the critical point.[36,37] From 20 °C down to 8 °C, a monotonic increase in the static birefringence is also observed (results not shown). This is due to the anisotropic scattering of light by microscopic polystyrene-rich or polyisoprene rich long-living microdomains. This scattering has been studied in great detail elsewhere, in order to assess the dynamics of concentration fluctuations on the way to the ordering transition,[38] which is estimated to be located below 10 °C for the present PS-*b*-PI concentration in DOP.[39]

Figure 2 displays the flow curve, i.e., the shear viscosity plotted as a function of the shear rate, but obtained from steady stress sweep tests performed with a 1.3 mm sample thickness, for two temperatures corresponding to the fully disordered state ($T = 40$ °C), and the regime dominated by concentration fluctuations ($T = 15$ °C), as discussed above. The flow curve at $T = 15$ °C is rather complex but can be separated in five stress or shear rate regimes (see Figure 2). A first regime can be identified at low shear rates (regime A), where the shear viscosity exhibits a Newtonian plateau. Increasing the stress level above a corresponding critical shear rate $\dot{\gamma}_B = 10^{-3}$ s^{-1}, results in a shear thinning (regime B), where the shear viscosity drops by 1 order of magnitude to values smaller than the apparent zero shear viscosity measured at 40 °C. When the shear rate is further increased above $\dot{\gamma}_C = 0.5$ s^{-1}, a small shear thickening regime is observed, followed by a viscosity level-off (regime C). The latter is also evident when the viscosity is plotted against the applied shear stress (see for instance Figure 3).We note here that stress-controlled experiments are essential for resolving this regime.[11,26] A fourth regime (regime D) is entered for shear rates above $\dot{\gamma}_D = 1$ s^{-1}. In this second shear thinning regime, viscosity data overlap those obtained at $T = 40$ °C, for shear rates in excess of 10 s^{-1}. Both sets of data exhibit a power law behavior with an exponent approaching −1. At the highest stress levels reached experimentally, the viscosity is nearly constant and exhibits a plateau identified as regime E. Rheological data obtained with different shearing geometries showed good reproducibility. This is illustrated in Figure 3, where steady-state viscosity data collected during creep tests performed with two different sample thicknesses (solid squares and triangles correspond to 1.17 and 0.886 mm, respectively) are satisfactorily matching the viscosity data of Figure 2 which are recast in Figure 3 as a function of the applied shear stress. The steady-state viscosity measured during the step shear rate test carried out with the cone and plate geometry of the ARES strain control rheometer (see Figure 6) is also reported in Figure 3 (see solid star) and confirms that the shearing geometry does not significantly affect the rheological data. In addition, no meniscus indentation or distortion was observed at the rim of the sheared sample, and polarized light microscopy images show homogeneous textures with no bubbles or cracks. Shear fracture can thus be excluded, which is consistent with the absence of severe shear thinning in regime E.[40] In the next sections, we present the rheo-optical responses obtained during experiments (stress sweeps, creep tests, or step shear rates) performed in each regime.

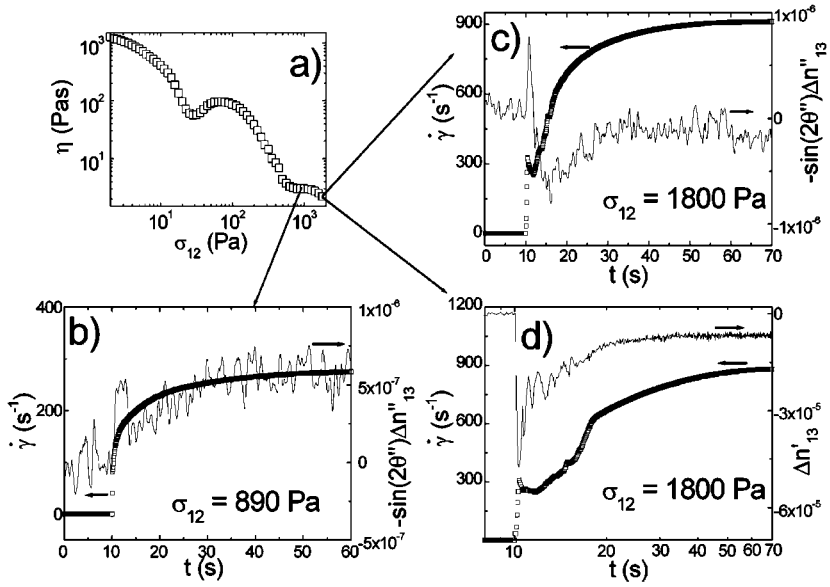

Figure 7. Shear viscosity, shear rate, dichroism first harmonic, and birefringence responses recorded in regime E for the PS-*b*-PI sample at $T = 15$ °C: (a) stress-dependent viscosity; (b) transient dichroism first harmonic and shear rate at 890 Pa; (c) transient dichroism first harmonic and shear rate at 1800 Pa; (d) transient birefringence and shear rate at 1800 Pa.

III.2. Regimes A and B. The shear-induced optical signals acquired at $T = 15$ °C simultaneously with the rheological data are plotted as a function of the applied shear stress in Figure 3. The viscosity data of Figure 2 are now plotted against stress.

Signals with amplitude larger than the detection limit of the rheo-optical experimental setup are first detected at stress levels close to roughly 10 Pa, which corresponds to the high shear rate limit of regime B, where a asymptotic power law with exponent −1 has been found in Figure 2. In this regime, inspection of the first and second harmonic signals, $-\sin 2\theta'' \Delta n''_{13}$ and $\Delta n''_{13} \cos 2\theta''$, respectively, allows for the explicit determination of both dichroism orientation and sign.[32] The dichroism is positive and oriented along the flow direction. The dichroism first harmonic plotted in Figure 3 first decreases and then reaches a local minimum at the onset of regime C. This result suggests that shear-induced structures with characteristic length scale of the order of the wavelength of the laser light are growing along the flow direction. This anisotropic shear-induced enhancement is further supported by the decrease of the transmitted light intensity detected for stress levels corresponding to the transition from regime B to regime C (see top curve in Figure 3).

The stress dependence of the stress-induced birefringence recorded at $T = 15$ °C is depicted in Figure 4a, along with the simultaneously recorded shear viscosity. A positive birefringence oriented along the flow direction emerges as the shear stress is increased from regime A to regime B. At higher stress levels in regime B, the birefringence saturates to a value of about 4.5×10^{-6}. This birefringence response is in qualitative agreement with the dichroism signal (Figure 3) and is roughly 1 order of magnitude larger than the latter. According to the Onuki−Doi theory,[41] a larger form birefringence is expected when the characteristic size of the structures scattering the light is smaller than the wavelength of the laser light. Indeed, polarized optical microscopy could not resolve any structure in regime B, thus indicating that the stress-enhanced concentration fluctuations which are responsible for the form dichroism possess a characteristic size smaller than the microscope resolution. Therefore, it appears that the birefringence signal measured in regime B originates from form contributions.

III.3. Regime C. Regime C, which is short-ranged, is characterized by a saturation in the dichroism first harmonic signal, followed by an increase which eventually results in a zeroing of the optical signal (see Figure 3). Note that this saturation and zeroing correspond to the shear thickening regime and the subsequent second viscosity plateau. The small disparity between changes in the optical and mechanical signals is attributed to the different effective shear rates in the two cases, as two different shear planes and flow locations are probed.[42]

The flow birefringence associated with regime C is less clear: given the noise in the optical signal (see Figure 4a), a nearly constant birefringence seems to correlate with the thickening behavior, whereas an increase in positive birefringence (by about 1×10^{-6}) is seen to accompany the onset of the viscosity plateau following the shear thickening. This is in sharp contrast to the zeroing of both dichroism and turbidity signals in this range of stresses. However, comparison of dichroism and birefringence data helps in separating form and intrinsic effects. On the basis of the fact that anisotropic scattering of the transmitted light is suppressed by stresses ranging from 70 to 150 Pa (see Figures 3 and 4a, end of regime C and onset of regime D), we may argue that form effects do not contribute to the flow birefringence recorded in this regime. We are then left with intrinsic contributions as the basic source of flow birefringence. Additional experiments performed at a temperature in the homogeneous region ($T = 40$ °C) where no concentration fluctuations were resolved (see also Figure 1) are presented in Figure 4b to further support this interpretation. A Newtonian viscosity is followed by a first smooth shear thinning which is eventually accentuated at higher stresses; there is no stress−fluctuations coupling, and no shear thickening is resolved. Accordingly, a positive flow birefringence smoothly rises up as the disordered PS-*b*-PI chains orient along the shear direction. The fact that the birefringence is positive implies that polyisoprene blocks contribute more than polystyrene blocks to the overall intrinsic birefringence, as a result of an enhanced entanglement plateau modulus G^0_N (larger local stress on polyisoprene blocks) and a higher optical anisotropy of polyisoprene blocks.[43] At higher stresses, the overall birefringence goes through a maximum, which roughly corresponds to the change of slope in the shear thinning viscosity. Note that the value of the birefringence

maximum nearly matches the value of the birefringence measured for the same amount of stress at $T = 15$ °C (see Figure 4a). Then, the birefringence drops to negative values, suggesting that the polystyrene blocks contribute more to the optical signal. This is possibly due to the larger number of entanglements of the polystyrene blocks, which need more energy to orient along the flow. It is worth mentioning that at this temperature no shear-induced dichroism could be detected. A quantitative estimate of the intrinsic birefringence associated with the polyisoprene blocks for the level of stress reached in regime C is given below in the discussion.

The transient rheo-optical response corresponding to a creep test at 28.2 Pa is depicted in Figure 5a in order to gain a better understanding of the structural change in regime C. This stress level corresponds to the minimum in the stress dependence of the shear viscosity where the form birefringence dominates (see Figure 4a). Upon stress inception, the shear rate displays a sharp overshoot, followed by an undershoot, before reaching steady state. In contrast to that, the birefringence transient displayed in Figure 5a evolves smoothly toward its steady-state value, and visual inspection confirmed that the sample remained virtually homogeneous (no morphology could be observed in polarized optical microscopy under shear) in the velocity−vorticity plane. The difference between optical and mechanical responses is also observed at a stress level of 71 Pa, which corresponds to the end of the thickening regime and where a transition from form-dominated effects to intrinsic contributions characterizes the birefringence response (see the weak birefringence jump in Figure 4a). As shown in Figure 5b, the birefringence displays a first rapid up rise and slower monotonic increase toward steady state, whereas the shear rate transient displays a first overshoot and subsequent undershoot, followed by a second overshoot before reaching smoothly the steady state. We note however here that the birefringence probes structures developing in the velocity−vorticity plane and therefore rather relates to normal stress differences. As not all stresses are elastic, the birefringence signal is not expected to accurately match the shear viscosity transients. Still, the qualitative comparison between normal stress and rheo-optical transients is interesting and revealing. However, experimental limitations of the stress rheometer used in the rheo-optical setup do not allow a systematic comparison of optical data with normal stresses (see section III.4 and Figure 6). This will be addressed in the future using a transparent cone and plate geometry adapted to the ARES rheometer.

The birefringence relaxation after flow cessation was analyzed with a stretched exponential function, $\Delta n'_{13} = \Delta n'_{13,0} \exp(-t/\tau)^{\beta}$, where $\Delta n'_{13,0}$ is the amplitude of the birefringence and τ the characteristic relaxation time. The extracted relaxation times τ and shape parameters β are decaying functions of the applied shear stress and were found to vary from 90 to 70 s and from 0.8 to 0.65, respectively; these values are indicative of the shear-induced rearrangement[33] of light scattering objects into smaller objects.

III.4. Regime D. In this regime, the flow curve presents a second shear thinning: the steady shear viscosity falls down to viscosity values recorded in the fluctuations free regime (see the flow curve recorded at $T = 40$ °C in Figure 2, which virtually superimposes on the flow curve measured at $T = 15$ °C). The second shear thinning corresponds to the evolution of a positive dichroism oriented along the vorticity direction (see in Figure 3 the corresponding increase of the first harmonic signal). The characteristic length scale of the shear-induced structure associated with this dichroism is of the order of the wavelength of the laser light (632.8 nm) and is enlarged with stress, as suggested by the monotonic decrease in the transmission of the light (see top curve in Figure 3). In regime D, the birefringence decreases and eventually changes sign. The stress corresponding to this change of sign is roughly 360 Pa and does not correlate to any specific viscoelastic transition (Figure 4a). We speculate that this reflects the complex interplay between intrinsic contributions originating from polyisoprene and polystyrene blocks (with a mismatch in entanglement density).

The structure which develops under shear in regime D has been explored with step shear rate experiments performed at 3 s^{-1}. The transient normal stress response N1 (measured on the ARES strain controlled rheometer) is displayed in Figure 6a, along with the dichroism response recorded in a separate experiment performed on the DSR rheometer, with the autostrain option (allowing the control of the applied shear rate[44]). Upon inception of flow, the normal stress exhibits an overshoot followed by a monotonic decay to the steady state. Additional structural characterization is provided by the normal stress relaxation after flow cessation presented in Figure 6b, together with the dichroism relaxation. The semilog representation in Figure 6b shows that the optical and mechanical data display the same relaxation behavior characterized by two relaxation times. The rather fast relaxation of both normal stress and dichroism first harmonic (both signals relax to steady-state values within 10 s) is roughly 1 order of magnitude faster than the birefringence relaxation time analyzed for a stress level corresponding to the onset of thickening and of regime C.

III.5. Regime E. When the sheared sample crosses regime E, the dichroism first harmonic signal goes through a maximum and changes sign at higher stresses (see Figure 3). This transition toward negative values is to be compared with the smooth evolution of the second harmonic $\Delta n''_{13} \cos 2\theta''$ which remains positive (result not shown) and thus unambiguously demonstrates that the dichroism remains positive.[32,45] Therefore, the change of sign in the $-\Delta n''_{13} \sin 2\theta''$ signal originates from the change of sign in $\sin 2\theta''$ which underpins the dichroism reorientation toward the flow direction that occurs in regime E. In addition, the sample becomes increasingly turbid (see top curve in Figure 3). Upon flow cessation, the dichroism and the transmitted light intensity exhibit quite different relaxation behaviors: the dichroism first harmonic relaxation is very fast whereas the sample turbidity slowly disappears. The comparison of these two complementary optical data suggests that the shear-induced structure generated in regime D and reoriented along the flow direction in regime E loses its orientation rapidly upon flow cessation and eventually disappears.

A very short birefringence plateau marks the transition between regimes D and E (see Figure 4a). At higher stresses in regime E, the negative birefringence further increases. Upon flow cessation, the negative birefringence first rapidly changes sign and then slowly relaxes to zero. This behavior is reminiscent of the birefringence relaxation measured in the PS-DOP system under similar experimental conditions.[11]

The shear rate responses recorded together with their corresponding dichroism and birefringence transients, during creep tests performed at 890 and 1800 Pa are presented in Figure 7. Despite the level of noise in the rather weak optical signal of Figure 7b, a monotonic increase up to a steady-state positive value is resolved in the dichroism first harmonic transient, which is indicative of the buildup of a structure which orients along the vorticity axis. Accordingly, a monotonic increase toward steady state is also displayed in the time dependence of the shear rate. The absence of overshoot in both the mechanical and the optical responses is in harmony with the apparent viscosity plateau observed for this shear stress level (see Figure 7a).

In the ultimate viscosity plateau regime, the optical and mechanical responses to a step shear stress of 1800 Pa are qualitatively different, as illustrated in Figure 7c. The stress start-up is accompanied by an immediate positive increase of the dichroism first harmonic signal, followed by a fast sign reversal,

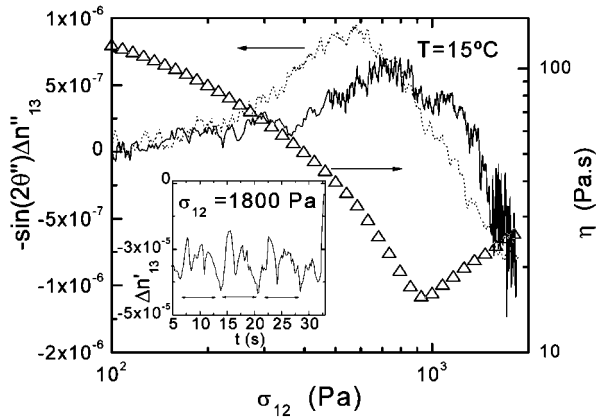

Figure 8. Steady-state rheo-optical response of a PS-DOP solution at $T = 15$ °C: viscosity−stress rheogram (△) and corresponding stress-induced dichroism first harmonic measured in situ. The dotted line represents the dichroism first harmonic signal measured with the PS-*b*-PI solution in regimes D and E (see Figure 3). Inset: birefringence transient recorded during the last step (1880 Pa) of a separate stress sweep; horizontal arrows indicate the temporal periodicity of the birefringence.

indicative of a rapid structural reorientation. A negative undershoot follows, as the optical signal approaches its final steady state. The shear rate data also exhibit an overshoot upon stress inception, which seems to be temporally correlated to the optical positive overshoot. On time scales corresponding to the optical negative undershoot, the shear rate transient is complex, before smoothly reaching its steady-state value (Figure 7c). Figure 7d presents complementary flow birefringence data obtained during a creep test performed at 1800 Pa, but with a larger gap (1.3 mm vs 1 mm) than in Figure 7c. The shear rates in Figure 7c,d are slightly different, which suggests that wall slip occurs (note that all creep tests are performed 30 min after sample loading, which is enough time for the full relaxation of the optical signals indicating the relaxation of the fluid). The extrapolation length computed from the shear rates and the sample thicknesses is of the order of 5 μm, which indicates that slip has a negligible quantitative effect on the rheo-optical response and has no qualitative influence on the results observed in regime E. The birefringence signal is negative, which suggests the dominance of intrinsic contributions originating from the polystyrene blocks. A sharp overshoot shows up at time scales corresponding to the shear rate one, whereas a relaxation in the birefringence signal toward the steady state accompanies the shear rate progressive increase toward steady state. This rheo-optical transient is qualitatively similar to the one displayed by a PS-DOP solution submitted at 15 °C to a creep of 1200 Pa.[11] To further check for structural similarity, the dichroism first harmonic recorded in regimes D and E, and which probes length scales larger than the intrinsic birefringence, was compared with the dichroism first harmonic recorded under equivalent conditions with a semidilute PS-DOP solution (with polystyrene molar mass $M_w = 2 \times 10^6$ g/mol) at $T = 15$ °C. This temperature is below the theta temperature (21 °C) of the PS-DOP solution. The polystyrene concentration is 8 wt %, which corresponds to roughly 25 effective entanglements. The comparison is displayed in Figure 8, where the dichroism first harmonic of Figure 3recorded in regimes D and E has also been reproduced (dotted line). A shear thinning, which is associated with the anisotropic growing along the vorticity of shear-induced polystyrene-rich domains giving rise to a positive increase of the dichroism first harmonic, dominates the rheo-optical response of the PS-DOP solution. This behavior is in harmony with earlier rheo-optical experiments where a positive form dichroism oriented along the vorticity and a butterfly pattern in light scattering have been reported.[2]

At higher stresses, shear thickening is observed as the polystyrene-rich domains rearrange into macroscopic (visible to the naked eye) stringlike structures oriented along the flow direction. This structural rearrangement is captured by the change of sign in the first harmonic signal. In the so-called "strong thickening" region,[11] the dichroism first harmonic exhibits temporal fluctuations which are associated with the development and breakup of the shear-induced turbid rings extended over the whole sample thickness and which are traveling outward the plates along the vorticity direction. These sustained temporal and spatial fluctuations are also resolved in the birefringence signal (see the inset in Figure 8 recorded during the last stress step of the stress sweep) as the turbid rings pass through the laser beam. Note that a period of nearly 7 s can be extracted from the transient displayed in Figure 8. This result conforms to the periodicity seen earlier in both mechanical and optical transients[11] obtained under similar experimental conditions.

IV. Discussion

Before analyzing in detail the rheo-optical responses observed in each regime and discussing the interplay between the shear-induced structures and the rheological behavior of the PS-*b*-PI solution, we should give here some general comments on the origin of the shear-induced optical signals, namely the birefringence and the dichroism.

Static birefringence is often used to determine the DOT in diblock copolymer melts and solutions.[46,47] As the ordered phase is approached, two sources for the depolarization of the transmitted light contribute to the overall increase of the birefringence signal. The first source, the static intrinsic birefringence, originates from the molecular optical anisotropy of polymer chains which are stretched by the lamellar or cylinder microstructure. The second contribution is the static form birefringence, which arises from the anisotropic scattering of transmitted light by ordered domains, where the refractive index is spatially modulated; as such, it exhibits similarities with the linear conservative dichroism. The relative magnitudes of the two contributions depend on the chemical nature of the polymeric blocks. For PS-*b*-PI ordered samples, the rather big contrast between the polyisoprene and polystyrene refractive indexes lead to large form contributions.[48] In particular, for a single crystal made of perfectly segregated cylinders with uniformly distributed solvent, the static form birefringence with respect to the cylinder long axis is positive and of the order of 10^{-4}.[48,24] As mentioned above, we noticed a monotonic increase in the static birefringence of the PS-*b*-PI sample from 5×10^{-7} (noise level of the experimental setup) up to 7×10^{-5}, upon cooling from 40 °C down to 8 °C. This may be attributed to static form effects arising from the growth of long-living concentration fluctuations, as the sample undergoes a transition toward an ordered phase of hexagonally packed PS-*b*-PI cylinders (HPCs) below 10 °C.[38,39] When shear stress is imposed on the PS-*b*-PI solution at $T = 15$ °C, we may expect the development of flow-induced form birefringence in a way similar to that measured for the linear conservative dichroism. Alternatively, disordered PS-*b*-PI copolymer chains can be oriented by the shear flow, thus giving rise to a flow-induced intrinsic birefringence which is not expected to obey a simple stress optical rule.[49] Rather, the overall shear-induced intrinsic birefringence results from the additive contributions from the polyisoprene and polystyrene blocks, which locally support a stress that differs from the macroscopically imposed one (see below for a quantitative estimate of shear-induced intrinsic birefringence caused by polyisoprene blocks). Each local stress weighted by the corresponding stress optical coefficient[50] represents the block contribution to the total birefringence. As

a result, the latter can be either positive or negative, since stress optical coefficients of polyisoprene and polystyrene are opposite in signs. It is thus clear that the interpretation of shear-induced birefringence is complex, as single PS-*b*-PI chains, concentration fluctuations, and fully oriented phase separated domains may contribute to the recorded signals.

However, a systematic comparison of shear-induced birefringence and dichroism signals should help in assigning the origin of the former. The dichroism originates from the anisotropic scattering of light by structures having a characteristic size of the order of the wavelength of the laser (632.8 nm) used to illuminate the sheared sample. Concentration fluctuations in a quiescent disordered diblock copolymer usually involve length scales of the order of one radius of gyration.[28,37,38] Therefore, dichroism is not likely to be measured on the static PS-*b*-PI solution. This picture can be drastically changed when shear stress is applied: the flow curve presented in Figure 2 suggests that shear rates in excess of $\dot{\gamma}_B$ are sufficient to affect concentration fluctuations. As a result, one might envision the stress-induced rearrangement of fluctuations into anisotropic structures with sizes spanning hundreds of nanometers, thus giving rise to substantial dichroism.

IV.1. Regime B. This regime is characterized by a first shear thinning behavior which is accompanied by the emergence of both shear-induced birefringence and dichroism for shear rates larger than $\dot{\gamma}_B$. The value of the latter (10^{-3} s^{-1}) is of particular interest, since it nearly matches the inverse relaxation time extracted at $T = 15$ °C from the intersection between the slopes 1 and 2 describing the terminal behavior of the loss (G'') and storage (G') moduli, respectively (see G' and G'' in the inset of Figure 2). This suggests that the shear thinning corresponds to a regime where PS-*b*-PI chains have sufficient mobility to couple to the shear flow due to the fact that the flow time is faster than the terminal time of the copolymer solution. At the highest shear rates reached in regime B, a change of slope in the shear rate dependence of the viscosity is observed: a power law with an exponent −1 is virtually reached, which is typical of entangled systems.[51,52] The exponent of the power law behavior and the low values of the viscosity in regime B (the viscosity drops below the value of the zero shear viscosity recorded at 40 °C) are reminiscent of the theoretical results of Onuki.[28] In Onuki's theory, the excess viscosity $\Delta\eta$ associated with concentration fluctuations in entangled symmetric copolymer chains, made of N links and N_e links between entanglements, is predicted to decay with the shear rate $\dot{\gamma}$ as

$$\Delta\eta = \frac{\eta_0}{90\pi}[f(1-f)]^{-3/4}N_e N^{-3/2}(\tau_{rept}\dot{\gamma})^{-1} \quad (1)$$

where η_0 is the viscosity of the fluctuations-free copolymer and τ_{rept} is the reptation time of disordered copolymer chains. Equation 1 is only valid for shear rates smaller than a critical value Γ_C written as $\Gamma_C \approx [3f(f-1)]^{-1}\tau_{rept}^{-1}$ and shows that $\Delta\eta$ decreases down to values smaller than η_0. This shear regime is explained by the anisotropic stretching of fluctuations in the shear plane[15,28] normal to the vorticity direction, which eventually results in the formation of a shear-induced ordered phase. On the basis of a rough estimation of τ_{rept} using the WLF temperature dependence of shift factors a_T and the longest relaxation time obtained at $T = 40$ °C, a value of 10^{-1} s^{-1} is computed for Γ_C at 15 °C. This suggests that the results displayed in Figure 2 are in qualitative agreement with Onuki's prediction. We also note that Γ_C nearly coincides with the frequency where the phase angle exhibits a minimum (see Figure 1), which has been assigned to relaxation modes originating from concentration fluctuations.[21] Rheo-optical data are also in harmony with these theoretical predictions: both form birefringence and dichroism are oriented along the flow (see regime B in Figures 3 and 4a). In addition, the saturation in both signals observed at stress levels corresponding to the viscosity plateau separating regimes B and C is a strong indication of a shear-induced DOT. On the basis of the HPCs morphology exhibited at equilibrium by the PS-*b*-PI copolymer solution,[38,39] the shear-induced ordered phase is expected to consist of HPCs oriented along the flow direction. Such a dynamic phase transition was observed for asymmetric copolymer melts[18] or low molecular mass (M_w being about 10^4 g/mol) asymmetric PS-*b*-PI solutions in DOP.[19,20] However, no rheological data were reported. The value of the birefringence displayed in Figure 4a is more than 1 order of magnitude smaller than the value expected for a perfectly oriented ordered phase made of strongly segregated HPCs.[24,48] This disparity could be attributed to the weak segregation of HPCs in the shear-induced phase,[48] the nonperfect alignment of the microstructure (for example, defects in the microstructure alignment generate some scattering of the light[53]), and/or the nonuniform dispersion of the solvent[24] which could weaken the optical contrast between unlike copolymer blocks. Note that intrinsic negative birefringence contributions arising from the polystyrene blocks are more than 1 order of magnitude smaller than the recorded birefringence displayed in Figure 4a for the corresponding stress level[11] and can thus be neglected. We also note here that data reported in Figure 4a were obtained at $T = 15$ °C, which is nearly 6 °C below the theta point of DOP for polystyrene chains, and that the formation of cylindrical micelles was recently reported[54] for asymmetric diblock copolymers in selective solvents for styrene. The smaller optical contrast between the micelles and the solvent[24,54] can explain the reduced form birefringence. Therefore, we may speculate that the saturation in both birefringence and dichroism signals (regimes B and C) corresponds to the full orientation along the flow direction of cylindrical micelles of PS-*b*-PI in DOP, resulting in a viscosity plateau which is the rheological signature of this new ordered phase.

IV.2. Regime C. When this ordered phase is further sheared, regime C is entered which is characterized by the loss of dichroism and a corresponding shear thickening (see Figure 3). A shear-induced reorientation of PS-*b*-PI cylindrical micelles along the shear gradient direction (homeotropic orientation[46]) would lead to such an optically isotropic morphology opposing resistance to the flow. However, this shear-induced morphology does not comply with the nonzeroing of the positive birefringence in regime C. Intrinsic contributions from polyisoprene blocks are called for explaining such behavior, as form contributions related to dichroism are vanishing. To check the validity of this interpretation, we may use an approximated stress optical rule, based on the assumption that the polyisoprene blocks are the only source of optical anisotropy, in order to give an estimate of the amount of intrinsic birefringence expected at stress levels where regime D initiates with a local viscosity plateau. Because of the nature of the experimental setup (the shear stress is measured in a plane perpendicular to the plane of birefringence), a modified stress optical rule is to be used:[11] $\Delta n'_{13} = 2C_{PI}\eta\tau_{rept}\dot{\gamma}^2$, where η and $\dot{\gamma}$ are the viscosity and the shear rate measured at the viscosity plateau resolved in regime D, C_{PI} is the stress optical coefficient for polyisoprene (taken as 2×10^{-9} Pa^{-1} [42]), and τ_{rept} is the longest relaxation time of the PS-*b*-PI chains introduced in eq 1. This yields an intrinsic birefringence, $\Delta n'_{13} = 4.6 \times 10^{-6}$, which is in fairly good agreement with the experimental birefringence displayed in Figure 4a at stresses of the order of 100 Pa. Therefore, we propose the following interpretation for the birefringence evidenced in regime C: from 30 to 60 Pa the form contributions dominate the constant birefringence signal; at higher stresses, intrinsic contributions become important and originate from the polyisoprene blocks, resulting in a net increase in the total

birefringence. However, a clear picture of the shear-induced morphology underlying the shear thickening behavior in regime C is still missing.

The second overshoot displayed by the shear rate transient in Figure 5b resembles the stress transient behavior observed in viscoelastic fluids such as nondilute polymer solutions and polymer mixtures and is identified with the mechanical signature of shear-induced phase separation or demixing.[55] We recently observed a second overshoot in the shear stress response of a thickening semidilute entangled polystyrene solution.[11] It was assigned to the stretching of polystyrene chains in shear-elongated polymer-rich domains. Accordingly, the intrinsic birefringence arising from the optical anisotropy in polystyrene chains displayed a transient similar to the stress transient. Sustained or damped oscillations in the mechanical signal which are mirrored in the optical response were also reported for shear banding fluids[26,56] where the stress couples to the shear-induced structures to give rise to flow instability[57] or rheo-chaos.[12,58] In particular, for stress-controlled experiments, bands developing in the vorticity direction are expected to give rise to a shear thickening similar to the one observed in Figure 2.[26,56] However, the transients displayed in Figure 5 suggest that such vorticity banding instability does not occur in regime C as the mechanical overshoot and undershoot are not mirrored in the birefringence signals. Similarly, the lack of temporal oscillations in the birefringence response rules out any transition from alignment to tumbling of the micellar PS-*b*-PI cylinders, as recently observed with shear thickening nematic colloidal suspensions of rodlike *fd* viruses.[59]

The birefringence relaxation shows that the ordered PS-*b*-PI micelles obtained in regime B are rearranged into smaller objects exhibiting a faster birefringence relaxation upon flow cessation. This is in agreement with the quantitative analysis of the birefringence which indicates that the shear thickening relates to a transition from form birefringence to intrinsic birefringence. Furthermore, both shear thickening and birefringence transition coincide with the disappearance of the solution turbidity, as evidenced by the total light intensity (see Figure 3), which recovers the value measured in regime A. We therefore speculate that the shear thickening in regime C corresponds to a complex disordering of the shear-induced ordered phase achieved in regime B into an homogeneous solution of disordered PS-*b*-PI chains exhibiting a larger viscosity and a net positive intrinsic birefringence. Though the loss of spatial correlation could not be captured by polarized optical microscopy (see section III.3), more insight into this issue could be gained by complementary in-situ light scattering experiment which shall be planned in the future.

IV.3. Regime D. The similarity in the flow curves measured at 15 and 40 °C (see Figure 2) indicates that the strongly nonlinear regime D is essentially caused by stress-induced local deformation and orientation where concentration fluctuations are not involved, as expected from Onuki's theoretical arguments:[28] for shear rates in excess of Γ_C, a non-Newtonian behavior exclusively caused by molecular deformation is expected, as fluctuations are suppressed in the flow direction. The monotonic decrease in the positive birefringence and the subsequent change of sign at higher stresses in regime D are in qualitative agreement with the birefringence measured at $T =$ 40 °C (compare parts a and b of Figure 4). This behavior has been explained by the complex interplay between intrinsic contributions arising from elastic polyisoprene blocks and polystyrene blocks (see section III.3).

However, the detection of both increasing dichroism and decreasing total light intensity does not comply with the picture of a sheared homogeneous PS-*b*-PI solution with copolymer chains aligning along the flow direction, as suggested by both flow curve and birefringence response. Rather, it indicates that a new structure is developing under flow. The rheo-optical transients in Figure 6 underline the difference between this shear-induced structure and the ordered phase obtained in regime B through the coupling between stress and concentration fluctuations. Upon flow cessation, the structural relaxation in regime D (see Figure 6b) is a much faster process than the one associated with the relaxation of the birefringence at the viscosity minimum in the range between regimes B and C. A faster relaxation suggests that concentration fluctuations affected by the shear in regime B are not involved in regime D. This, in turn, implies that a shear rate of 3 s^{-1} is strong enough to suppress these fluctuations, as expected from theoretical arguments for $\dot{\gamma} > \Gamma_C$ (a value of 10^{-1} s^{-1} has been computed for the latter; see section IV.1). We could then propose that the suppression of fluctuations costs an elastic penalty which is reflected in the normal stress overshoot displayed in Figure 6a. However, a clear characterization of the shear-induced structure which develops at longer time and correlates to the positive increase of the dichroism is still missing.

IV.4. Regime E. In regime E, the structure that emerged in regime D reorients toward the flow direction. This reorientation process is captured by the dichroism response, which nicely matches the rheo-optical behavior of a PS-DOP solution sheared under similar conditions (see the comparison in Figure 8). However, comparison of Figures 7 and 8 also reveals qualitative and quantitative differences among the structures developed in the high shear stress regimes of the PS-*b*-PI and the PS-DOP systems. First, the temporal fluctuations evidenced in the PS-DOP system (inset in Figure 8) are not observed for the PS-*b*-PI solution (see Figure 7d), and second, no shear thickening shows up in the high shear stress region of the PS-*b*-PI flow curve. We further note that for a shear stress of 1000 Pa the PS-DOP viscosity is nearly 10 times higher than the PS-*b*-PI viscosity, and the intrinsic negative birefringence associated with the PS chains is roughly 3 times larger than the intrinsic birefringence associated with the polystyrene blocks in the PS-*b*-PI. This quantitative mismatch could be explained by the fact that the PS-*b*-PI copolymer chains are less entangled than the polystyrene chains of the same total molecular mass. Both qualitative and quantitative discrepancies point to the fact that in the copolymer solution shear-induced copolymer rich domains are arranged in a string structure, which remains stable under imposed stress and where PS blocks are less extended than in the PS-DOP solution. For the latter, the critical shear rate for the onset of shear thickening is an increasing function of the sample thickness.[11] This result is at odds with experiments and theoretical arguments[60] describing purely elastic flow instabilities in parallel plate geometry: the critical shear rate for the onset of such instabilities varies inversely with the gap. Thus, the oscillatory rheo-optical transients should not relate to an elastically driven flow instability.

Sustained temporal and spatial oscillations have been recently generated by a simple shear thickening model[27] that couples the imposed stress to relaxing structural modes which are slower than the longest linear stress relaxation of the fluid. On the basis of the theoretical arguments proposed in this model, the absence of shear thickening and associated sustained temporal fluctuations in the rheo-optical behavior of the PS-*b*-PI solution is due to the fact that the characteristic relaxation time of the string structure (estimated to roughly 300 s, based on the birefringence relaxation upon shear cessation in Figure 4a) is not slow enough when compared to the longest stress relaxation time in the quiescent PS-*b*-PI solution (the data of Figure 2 suggest a time of 900 s). In contrast, the quiescent PS-DOP solution shows a much faster linear stress relaxation (the latter is 0.6 s as determined in ref 11 and is associated with reptation dynamics)

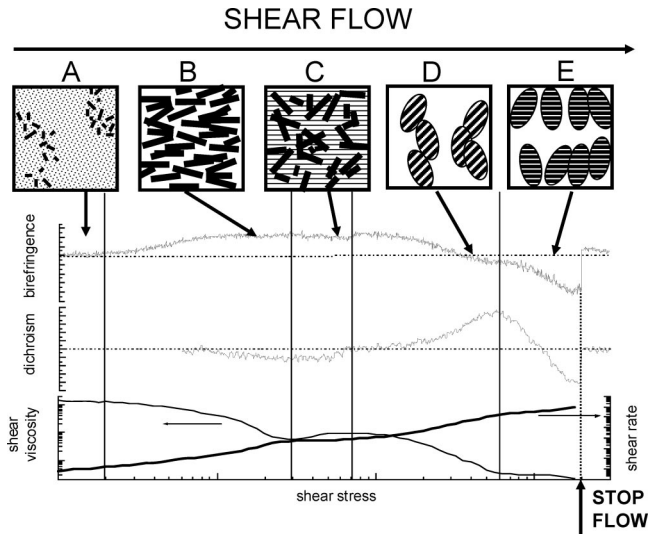

Figure 9. Sketch representing the proposed shear-induced structures giving rise to the linear conservative dichroism, the flow birefringence, the shear viscosity, and the steady-state shear rate resolved in the different stress regimes. Rods displayed in cartoons A, B, and C represent micellar PS-*b*-PI cylinders, whereas hatched droplets in charts D and E represent total polymer concentration fluctuations containing PS-*b*-PI chains aligned along the flow. The backgrounds in cartoons A and C represent homogeneous disordered and aligned PS-*b*-PI chains in DOP, respectively, whereas white backgrounds in cartoons B, D, and E represent DOP.

when compared to the characteristic time of the string structure which is known to relax over a period of roughly 7 s (see inset in Figure 8). Therefore, the enthalpic effects associated with the microsegregated domains which slowly fluctuate when the DOT is approached, seem responsible for the absence of shear thickening and related flow instability in regime E.

IV.5. Emerging Picture of Flow-Fluctuations Coupling. The rheo-optical responses presented above are compiled in Figure 9, along with simple cartoons illustrating the proposed shear-induced structures associated with each stress regime. The dynamics of the quiescent PS-*b*-PI solution is essentially governed by the concentration fluctuations which could be considered as long-lived ordered domains in the copolymer solution.[38] At low shear stresses corresponding to regime A, these domains (pictured as regions of thin rods representing PS-*b*-PI cylindrical micelles with isotropic orientations in cartoon A) are not affected by the flow field as sufficient time is left for their relaxation under flow. At higher shear stress, the domains are effectively deformed and forced to align along the flow,[28] as the characteristic time of the shear flow is faster than the relaxation time of the concentration fluctuations. The structural change occurring in this stress region (regime B) results in a drop of the viscosity and an increase in the anisotropic scattering of the light. The latter causes the emergence of both linear conservative dichroism and form birefringence oriented along the flow direction. A further increase of the stress leads to a shear rate dependence of the viscosity characterized by a power law behavior with exponent −1, in qualitative agreement with theoretical predictions of Onuki.[28] In this range of stresses, the enhanced concentration fluctuations are oriented in the velocity direction, as evidenced by the saturation of the birefringence signal. At the highest stress applied in regime B, a viscosity plateau (or minimum) is resolved, concurrently with the saturation of both dichroism and total transmitted light intensity. This rheo-optical behavior signifies the shear-induced DOT, which is typical of asymmetric diblock copolymers.[17–20] We speculate that the viscosity minimum in regime B is associated with the alignment along the flow direction of shear enhanced micellar PS-*b*-PI cylinders in solution with DOP. This stress-induced structure (pictured in cartoon B with larger rods than in cartoon A) bears some evident morphological similarities with sheared colloidal suspensions,[61,62] which usually exhibit a shear thickening behavior in strong flows.

Therefore, the thickening regime encountered at higher stresses comes as no surprise (regime C). However, the mechanism that leads to the increase in shear viscosity seems to be different from suspensions. In colloids, the formation of transient clusters under shear is responsible for the observed increase in both dichroism magnitude and viscosity,[61] as hydrodynamic interactions are increased.[62] The shear thickening evidenced in regime C relates to a dramatic reduction of shear induced dichroism to values beyond experimental detection and a disappearance of turbidity, whereas the form birefringence decreases to values below those corresponding to purely intrinsic polyisoprene contributions. This regime corresponds to a loss of structural order (in the flow direction), which in turn results in a viscosity up rise. The loss of spatial correlation is further supported by the second overshoot observed in shear rate transients and the faster birefringence relaxation upon shear cessation which indicates that the shear-induced structure has been rearranged into smaller objects.[33] Therefore, in this regime, an homogeneous diblock copolymer solution results from the stress-induced breakup of unstable micellar PS-*b*-PI cylinders (see also onset of regime D). We note here that a model describing flow−concentration coupling captures such a shear thickening behavior but is associated with a phase transition toward unstable layers.[63] Indeed, flow−concentration coupling is important since the rheo-optical response measured in regimes D and E suggests that concentration fluctuations are shear-enhanced and that the system is driven toward dynamic phase separation, in a way similar to the one found for semidilute polymer solutions below the theta temperature (cartoons D and E in Figure 9). However, no shear thickening regime and flow instability characterized by periodic rheo-optical signals[11] could be resolved with the PS-*b*-PI. A recent model[27] coupling nonlinear rheology and slow structural relaxation provides an explanation to our results. The longest relaxation time in the quiescent PS-*b*-PI solution (roughly 900 s) is too slow when compared to the relaxation time of the structure induced in regime E (roughly 300 s) or of the structure induced in regime B (roughly 90 s). In this case, no vorticity banding instability can develop.

V. Concluding Remarks

Stress−fluctuations coupling gives rise to a rich rheological response which encompasses shear thinning, shear thickening, and vorticity banding instability.[64] Shear thinning is the signature of the anisotropic enhancement of concentration fluctuations along the flow direction, as seen with the disordered and entangled PS-*b*-PI solution, or along the vorticity direction as observed with the entangled PS-DOP solution and with the homogeneous PS-*b*-PI solution sheared below the theta temperature. Stress enhancement of concentration fluctuations eventually results in the buildup of ordered phases oriented in a preferred direction and possessing slow or fast structural relaxation. The rheological signature of the stress-induced phase transition is a Newtonian plateau (resolved at the highest stress regime in the PS-*b*-PI solution), when the shear-oriented phase shows fast structural relaxation which occurs on a shorter time scale than the longer stress relaxation of the quiescent fluid. In contrast, spatio-temporal fluctuations in both stress-induced structure and shear rate give rise to shear thickening. This type of vorticity banding instability occurs when the shear-induced phase exhibits long structural memory which relaxes on a much

slower time scale than the slowest linear stress relaxation mode in the quiescent fluid. In addition to the PS-DOP solution, examples of complex fluids with such slow structural memory and fast linear stress relaxation include wormlike surfactant solutions[13,57] and lyotropic lamellar phases.[12] All these systems exhibit shear bands which are traveling along the vorticity direction and result in mechanical periodic signals similar to the ones recently computed with a minimal model for shear thickening fluids.[27]

References and Notes

(1) Lodge, T. P. *Macromol. Chem. Phys.* **2003**, *204*, 265–273.
(2) Fuller, G. G. *Optical Rheometry of Complex Fluids*; Oxford University Press: New York, 1995.
(3) Kornfield, J. A.; Kumaraswamy, G.; Issaian, A. M. *Ind. Eng. Chem. Res.* **2002**, *41*, 6383–6392.
(4) Jackson, C. L.; Barnes, K. A.; Morrison, F. A.; Mays, J. W.; Nakatani, A. L.; Nakatani, A. I.; Han, C. C. *Macromolecules* **1995**, *28*, 713–722.
(5) Callaghan, P. T. *Curr. Opin. Colloid Interface Sci.* **2006**, *11*, 13–18.
(6) Yanase, H.; Moldenaers, P.; Mewis, J.; Abetz, V.; van Egmond, J.; Fuller, G. G. *Rheol. Acta* **1991**, *30*, 89–97.
(7) Wu, X. J.; Pine, D. J.; Dixon, P. K. *Phys. Rev. Lett.* **1991**, *66*, 2408–2411.
(8) Kume, T.; Hashimoto, T.; Takahashi, T.; Fuller, G. G. *Macromolecules* **1997**, *30*, 7232–7236.
(9) Helfand, E.; Fredrickson, G. H. *Phys. Rev. Lett.* **1989**, *62*, 2468–2471.
(10) van Egmond, J. W. *Macromolecules* **1997**, *30*, 8045–8057.
(11) Hilliou, L.; Vlassopoulos, D. *Ind. Eng. Chem. Res.* **2002**, *41*, 6246–6255.
(12) Salmon, J.-B.; Colin, A.; Roux, D. *Phys. Rev. E* **2002**, *66*, 031505.
(13) Fischer, P.; Wheeler, E. K.; Fuller, G. G. *Rheol. Acta* **2002**, *41*, 35–44.
(14) Leibler, L. *Macromolecules* **1980**, *13*, 1602–1617.
(15) Cates, M. E.; Milner, S. T. *Phys. Rev. Lett.* **1989**, *62*, 1856–1859.
(16) Fredrickson, G. H. *J. Rheol.* **1994**, *38*, 1045–1067.
(17) Koppi, K. A.; Tirrell, M.; Bates, F. S. *Phys. Rev. Lett.* **1993**, *70*, 1449–1452.
(18) Almdal, K.; Mortensen, K.; Koppi, K. A.; Tirrell, M.; Bates, F. S. *J. Phys. II* **1996**, *6*, 617–637.
(19) Balsara, N. P.; Hammouda, B.; Kesani, P. K.; Jonnalagadda, S. V.; Straty, G. C. *Macromolecules* **1994**, *27*, 2566–2573.
(20) Balsara, N. P.; Dai, H. J. *J. Chem. Phys.* **1996**, *105*, 2942–2945.
(21) Jin, X.; Lodge, T. P. *Rheol. Acta* **1997**, *36*, 229–238.
(22) Hahn, H.; Lee, J. H.; Balsara, N. P.; Garetz, B. A.; Watanabe, H. *Macromolecules* **2001**, *34*, 8701–8709.
(23) Koppi, K. A.; Tirrell, M.; Bates, F. S.; Almdal, K.; Colby, R. H. *J. Phys. II* **1992**, *2*, 1941–1959.
(24) Zryd, J. L.; Burghardt, W. R. *Macromolecules* **1998**, *31*, 3656–3670.
(25) Hermel, T. J.; Wu, L. F.; Hahn, S. F.; Lodge, T. P.; Bates, S. F. *Macromolecules* **2002**, *35*, 4685–4689.
(26) Olmsted, P. D. *Europhys. Lett.* **1999**, *48*, 339–345.
(27) Aradian, A.; Cates, M. E. *Phys. Rev. E* **2006**, *73*, 041508.
(28) Onuki, A. *J. Chem. Phys.* **1987**, *87*, 3692–3697.
(29) Hadjichristidis, N.; Iatrou, H.; Pispas, S.; Pitsikalis, M. *J. Polym. Sci., Part A: Polym. Chem.* **2000**, *38*, 3211–3234.
(30) Sigel, R.; Pispas, S.; Hadjichistidis, N.; Vlassopoulos, D.; Fytas, G. *Macromolecules* **1999**, *32*, 8447–8453.
(31) Hilliou, L.; Vlassopoulos, D.; Rehahn, M. *Macromolecules* **2000**, *33*, 3105–3110.
(32) Hilliou, L.; Vlassopoulos, D.; Rehahn, M. *Macromolecules* **2001**, *34*, 1742–1750.
(33) Hilliou, L.; Vlassopoulos, D.; Rehahn, M. *Rheol. Acta* **1999**, *38*, 514–527.
(34) Wewerka, A.; Vierther, K.; Vlassopoulos, D.; Stelzer, F. *Rheol. Acta* **2001**, *40*, 416–425.
(35) Kannan, R. M.; Kornfield, J. A.; Schwenk, N.; Boeffel, C. *Macromolecules* **1993**, *26*, 2050–2056.
(36) Fredrickson, G. H.; Larson, R. G. *J. Chem. Phys.* **1987**, *86*, 1553–1560.
(37) Fredrickson, G. H.; Helfand, E. *J. Chem. Phys.* **1988**, *89*, 5890–5897.
(38) Holmqvist, P.; Pispas, S.; Hadjichristidis, N.; Fytas, G.; Sigel, R. *Macromolecules* **2003**, *36*, 830–838.
(39) Holmqvist, P.; Fytas, G. Private communication.
(40) (a) Larson, R. G. *Rheol. Acta* **1992**, *31*, 213–263. (b) Schweizer, T. *Rheol. Acta* **2007**, *46*, 629–637.
(41) Onuki, A.; Doi, M. J. *Chem. Phys.* **1986**, *85*, 1190–1197.
(42) (a) Shear rate values at the laser beam location are somehow lower than the shear rate values at the rim used to calculate the viscosity data (see the Experimental Section) and (b) viscosity data relate to rheological properties probed in the plane given by the velocity gradient and flow directions, whereas the optical properties are probed in a different shear plane, namely the plane made by vorticity and flow directions.
(43) Okamoto, H.; Inoue, T.; Osaki, K. *J. Polym. Sci., Part B: Polym. Phys.* **1995**, *33*, 417–424.
(44) A time lag of nearly 6 s was needed for the applied shear rate to reach a steady state. A similar time lag was applied to the complex dichroism transient upon flow inception. However, the steady-state viscosities recorded during both experiments are in harmony with the steady-state viscosity displayed in Figure 3 for the corresponding shear rate (viscosities of 51 and 54 Pa s were measured with the ARES and DSR rheometers, respectively), which indicates that regime D can be equally accessed under both stress and shear rate control.
(45) Lee, J.-D.; Yang, S.-M. *J. Colloid Interface Sci.* **1998**, *205*, 397–409.
(46) Balsara, N. P.; Perahia, D.; Safinya, C. R.; Tirrell, M.; Lodge, T. P. *Macromolecules* **1992**, *25*, 3896–3901.
(47) Lodge, T. P.; Pudil, B.; Hanley, K. J. *Macromolecules* **2002**, *35*, 4707–4717.
(48) Lodge, T. P.; Fredrickson, G. H. *Macromolecules* **1992**, *25*, 5643–5650.
(49) Lodge, T. P.; Lodge, S. A. *Rheol. Acta* **1992**, *31*, 32–43.
(50) Osaki, K.; Takatori, E.; Ueda, M.; Kurata, M.; Kotaka, T.; Ohnuma, H. *Macromolecules* **1989**, *22*, 2457–2460.
(51) Larson, R. G. In *The Structure and Rheology of Complex Fluids*; Oxford University Press: New York, 1999; p 163.
(52) Marrucci, G. *J. Non-Newtonian Fluid Mech.* **1996**, *62*, 279–289.
(53) Wang, H.; Newstein, M. C.; Chang, M. Y.; Balsara, N. P.; Garetz, B. A. *Macromolecules* **2000**, *33*, 3719–3730.
(54) Bang, J.; Jain, S.; Li, Z.; Lodge, T. P.; Pedersen, J. S.; Kesselman, E.; Talmon, Y. *Macromolecules* **2006**, *39*, 1199–1208.
(55) Larson, R. G. *Rheol. Acta* **1992**, *31*, 497–520.
(56) (a) Goveas, J. L.; Olmsted, P. D. *Eur. Phys. J. E* **2001**, *6*, 79–89. (b) Dhont, J. K. G.; Lettinga, M. P.; Dogic, Z.; Lenstra, T. A. J.; Wang, H.; Rathgeber, S.; Carletto, P.; Willner, L.; Frielinghaus, H.; Lindner, P. *Faraday Discuss.* **2003**, *123*, 157–172. (c) Kang, K.; Lettinga, M. P.; Dogic, Z.; Dhont, J. K. G. *Phys. Rev. E* **2006**, *74*, 026307. (d) Lin-Gibson, S.; Pathak, J. A.; Grulke, E. A.; Wang, H.; Hobbie, E. K. *Phys. Rev. Lett.* **2004**, *92*, 048302. (e) Vermant, J.; Solomon, M. J. *J. Phys.: Condens. Matter* **2005**, *17*, R187–R216.
(57) Wheeler, E. K.; Fischer, P.; Fuller, G. G. *J. Non-Newtonian Fluid Mech.* **1998**, *75*, 193–208.
(58) (a) Cates, M. E.; Head, D. A.; Adjari, A. *Phys. Rev. E* **2002**, *66*, 025202. (b) Fielding, S.; Olmsted, P. *Phys. Rev. Lett.* **2004**, *92*, 084502.
(59) Lettinga, M. P.; Dogic, Z.; Wang, H.; Vermant, J. *Langmuir* **2005**, *21*, 8048–8057.
(60) Shaqfeh, E. S. G. *Annu. Rev. Fluid. Mech.* **1996**, *28*, 129–185.
(61) d'Haene, P.; Mewis, J.; Fuller, G. G. *J. Colloid Interface Sci.* **1993**, *156*, 350–358.
(62) (a) Bender, J. W.; Wagner, N. J. *J. Colloid Interface Sci.* **1995**, *172*, 171–184. (b) Newstein, M. C.; Wang, H.; Balsara, N. P.; Lefebvre, A. A.; Watanabe, H.; Osaki, K.; Shikata, T.; Niwa, H.; Morishima, Y. *J. Chem. Phys.* **1999**, *111*, 4827–4838. (c) Melrose, J. R.; Ball, R. C. *J. Rheol.* **2004**, *48*, 937–960. (d) Frith, W. J.; d'Haene, P.; Buscall, R.; Mewis, J. *J. Rheol.* **1996**, *40*, 531–549. (e) Lee, Y. S.; Wagner, N. J. *Ind. Eng. Chem. Res.* **2006**, *45*, 7015–7024. (f) O'Brien, V. T.; Mackay, M. E. *Langmuir* **2000**, *16*, 7931–7938.
(63) Schmidt, V.; Marques, C. M.; Lequeux, F. *Phys. Rev. E* **1995**, *52*, 4009–4015.
(64) Dhont, J. K. G.; Briels, W. J. *Rheol. Acta* **2008**, *47*, 257–281.

MA702566N